



Trade Science Inc.

ISSN : 0974 - 7486

Volume 8 Issue 2

# Materials Science

An Indian Journal

Full Paper

MSAIJ, 8(2), 2012 [60-66]

## Effect of substrate temperature and concentration on spray deposited zinc oxide thin films

R.T.Sapkal<sup>1</sup>, S.S.Shinde<sup>1</sup>, A.R.Babar<sup>1</sup>, K.Y.Rajpure<sup>1</sup>, P.S.Patil<sup>2</sup>, C.H.Bhosale<sup>1\*</sup>

<sup>1</sup>Electrochemical Materials Laboratory, Department of Physics, Shivaji University, Kolhapur-416004, (INDIA)

<sup>2</sup>Thin Film Materials Laboratory, Department of Physics, Shivaji University, Kolhapur- 416004, (INDIA)

E-mail : bhosale\_ch@yahoo.com

Received: 7<sup>th</sup> July, 2011 ; Accepted: 7<sup>th</sup> August, 2011

### ABSTRACT

Zinc Oxide (ZnO) thin films have been deposited onto glass substrates by economical spray pyrolysis at different substrate temperatures and concentrations of Zinc acetate used as precursor under atmospheric pressure. The films were characterized by XRD, optical transmittance and SEM techniques. All the films are polycrystalline with hexagonal wurtzite structure, with c-axis growth (002) perpendicular to substrate surface. At the substrate temperature of 400°C and solution concentration of 0.2 M, ZnO thin films exhibited highest crystallinity. The grain size, Zn – O bond length, dislocation density and stress of the films changes from 72.26 nm to 105.33 nm., 1.9699 Å to 1.9725 Å,  $1.863 \times 10^{-4} \text{ (nm)}^{-2}$  to  $0.9032 \times 10^{-4} \text{ (nm)}^{-2}$  and -0.48798 Gpa to 55.066 Gpa respectively. Morphological study showed surface microrods are obtained at lower concentration (0.1M). Length and diameter of surface microrods were found in the range from 1 μm to 8 μm and 0.1 μm to 0.9 μm respectively. Optical band gap was found to be in the range 2.92 eV to 3.24 eV. The average transmission of the films is about 85% in the visible region.

© 2012 Trade Science Inc. - INDIA

### KEYWORDS

Spray pyrolysis method;  
XRD;  
Optical transmittance;  
SEM.

### INTRODUCTION

Zinc oxide is an n – type wide band gap (> 3 eV) semiconductive oxide<sup>[1]</sup>. Due to its conductivity and high transmittance, ZnO films have been attracting growing attention in the recent years. It has been recognized as one of the promising nanomaterials in a broad range of technological applications<sup>[2]</sup> e.g. surface acoustic wave device<sup>[3]</sup>, chemical sensor<sup>[4]</sup>, photonic crystal<sup>[5]</sup>, light emitting diodes<sup>[6]</sup> and solar cell<sup>[7]</sup>. ZnO thin films have been used as ozone gas sensors because they have high sensitivity to many gases<sup>[8]</sup>. In addition, a great deal of

attention has been focused on the study of low dimensional nanostructures of ZnO thin films<sup>[9]</sup>. Various methods have been used to grow ZnO nanostructures, such as nanorods<sup>[10-12]</sup>, microrods<sup>[13]</sup>, nanowires<sup>[14]</sup>, nanobelts<sup>[15]</sup> and nanostars<sup>[16]</sup>. The methods include radio frequency magnetron sputtering<sup>[17]</sup>, chemical vapor deposition<sup>[18]</sup>, thermal vaporization<sup>[19]</sup>, hydrothermal method<sup>[20]</sup>, sol-gel method<sup>[21]</sup>, laser ablation<sup>[22]</sup>, electrochemical deposition<sup>[23]</sup> and ion beam assisted deposition<sup>[24]</sup> and spray pyrolysis<sup>[25]</sup>. Among these methods, spray pyrolysis is a useful alternative to the traditional methods for obtaining thin films of pure ZnO. It is of

particular interest because of its simplicity, low cost and eco-friendly nature. Many researchers have prepared the ZnO thin films by spray pyrolysis technique in aqueous and non aqueous medium with and without addition of alcohol<sup>[26-28]</sup>. However very few researchers have paid attention to 'obtain ZnO microrod thin films through aqueous, non aqueous medium and their characterization. Here we report the direct growth of zinc oxide thin films on glass substrate by chemical spray pyrolysis method. We have also carried out structural, optical and morphological study of the films with the aim of understanding physical properties of obtained ZnO rods.

## EXPERIMENTAL

ZnO thin films were deposited by a locally made spray pyrolysis deposition chamber on to glass substrate (75 X 25 X 2 mm<sup>3</sup>) using zinc acetate as precursor. The solution of zinc acetate was prepared in water + methanol + acetic acid (25 cc + 65 cc + 10 cc)<sup>[29]</sup>. The films were prepared by varying the deposition temperature from 300°C to 450°C (0.1M, 0.2M, 0.3M and 0.4 M) and concentration of zinc acetate from 0.1 M to 0.4M (at 300°C, 350°C, 400°C and 450°C) in order to study the effect of substrate temperature and precursor concentration on properties of the films. Other parameters such as spray rate (5cc min<sup>-1</sup>), nozzle to substrate distance (33cm) and carrier air pressure (2 atm) were kept at their fixed value throughout deposition process. Glass substrates were ultrasonically cleaned by deionized water, acetone and methanol before the experiment.

The structural properties were studied by Philips X- ray diffractometer PW – 1710 ( $\lambda = 1.5405 \text{ \AA}$ ) using Cu – K $_{\alpha}$  radiation in the span of 20 to 80°. Surface morphology of the thin film was studied with JEOL JSM- 6360 Scanning Electron Microscope (SEM). Optical absorption study was carried out in the wavelength range 300 nm – 1000 nm using spectrometer Systronic model -119.

## RESULT AND DISCUSSION

### Structural properties

XRD patterns of ZnO thin films deposited at differ-

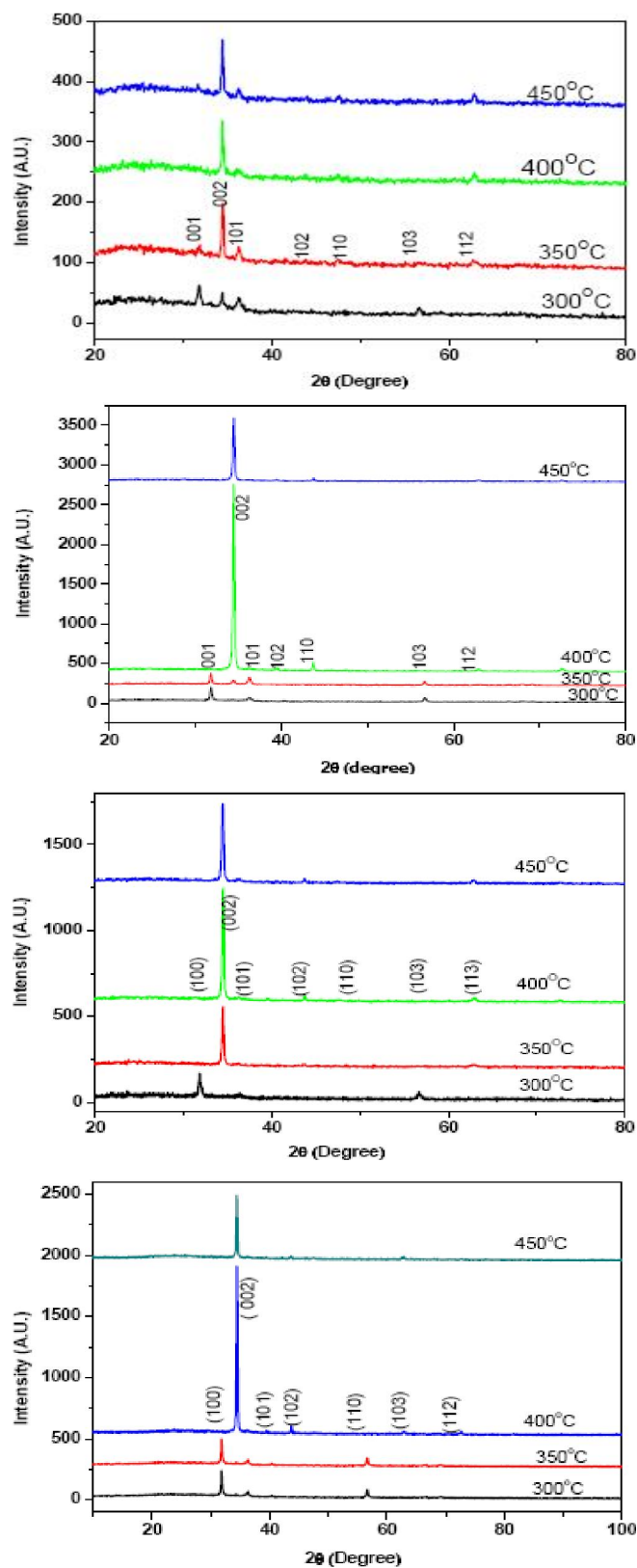


Figure 1 : XRD pattern of ZnO thin films deposited at different temperatures at (a) 0.1 M (b) 0.2M (c) 0.3 M (d) 0.4M concentration of zinc acetate.

## Full Paper

ent temperatures and concentrations are shown in Figure 1 (a-d) respectively. From XRD data, it is seen that the films exhibit hexagonal (Wurtzite) crystal structure with preferential growth along the (002) plane. The intensity of the (002) diffraction is highest at the substrate temperature of 400°C, indicating an improvement of the film crystallinity at this temperature. When substrate temperature 300°C many sputtered ions form the target, which cannot obtain enough energy to adjust the bound direction and length to the lattice position<sup>[30]</sup>.

Upon increasing the substrate temperature, crystallinity of the samples increased due possibility of homogeneous reactions. The analogous results were reported for spray deposited ZnO films, deposited through aqueous medium<sup>[31]</sup>. This was explained based on higher chemical purity of the ZnO films, which resulted from thermal decomposition. All the peaks in the diffraction pattern were indexed on the basis of a JCPDS data card 05 - 6044

The crystallite size of the ZnO thin films prepared at different temperatures and concentration was evaluated from the full width at half maxima (FWHM) of (002) peak using Scherrer's formula,

$$D = \frac{0.94\lambda}{\beta \cos \theta} \quad (1)$$

where  $\lambda$ ,  $\theta$  and  $\beta$  are X-ray wavelength, Bragg diffraction angle and FWHM respectively. The grain size obtain is 73.26 nm, 92.23 nm, 92.26 nm and 105.33 nm for the films deposited at 300°C, 350°C, 400°C and 450°C respectively. XRD studies revealed that optimized substrate temperature for the growth of ZnO film with preferred (002) orientation is 400°C.

The dislocation density  $\delta$  which represents the amount of defects in the film, was determined from the formula,  $\delta = 1/D^2$ <sup>[32]</sup>. The larger the D and smaller FWHM values indicate better crystallization of the film. It was observed that the grain size values increases with increasing deposition temperature and decreases with increasing concentration, which clearly reveals the deterioration in the crystallinity. These values are given in the TABLE 1. Dislocation density exhibit decreasing trend with increasing deposition temperature and increases as concentration increases, which leads decreasing of lattice imperfections as deposition temperature increases and increase of lattice imperfections as

**TABLE 1 : Position of (002) plane, FWHM, particle size, dislocation density, a/c ratio and Zn-O bond length at different temperatures and concentrations.**

Temperature	FWHM	$2\theta$	D (nm)	$\delta \times 10^{-4}$ (nm) <sup>-2</sup>	Thickness (nm)	L(A°)
3000C	0.1968	31.83	73.26	1.863	156	1.9699
3500C	0.1574	34.47	92.23	1.175	204	1.9756
4000C	0.1574	34.46	92.26	1.175	252	1.9655
4500C	0.1378	34.40	105.33	0.9032	116	1.9725
Concentration						
0.1M	0.1574	34.45	92.22	1.1758	125	1.9781
0.2M	0.1574	34.46	92.26	1.1747	252	1.9655
0.3M	0.1968	34.49	73.77	1.8375	304	1.9746
0.4M	0.1717	34.50	81.98	1.4879	415	1.9751

concentration increases.

Lattice constants a and c are calculated by using well known analytical method. Zn – O bond length L is given by formula<sup>[33]</sup>.

$$L = \sqrt{\frac{a^3}{3} + \left(\frac{1}{2} - u\right)^2 c^2} \quad (2)$$

Where the u parameter in the Wurtzite structure is given by,

$$u = \frac{a^2}{3c^2} + 0.25 \quad (3)$$

Zn- O bond length is given TABLE 1. It is observed that bond length is minimum of its value at 400°C and 0.2M concentration. Such film being relatively stable may have prospective applications in purification of water by photoelectrocatalysis.

Quantitative information concerning the preferential crystal orientation can be obtained from the texture coefficient, TC defined as,

$$TC(hkl) = \frac{\frac{I(hkl)}{I_0(hkl)}}{\frac{1}{n} \sum \frac{I(hkl)}{I_0(hkl)}} \quad (4)$$

Where TC (hkl) is the texture coefficient, I (hkl) is the XRD intensity and n is number of diffraction peaks considered,  $I_0$  (hkl) is the intensity of the XRD reference of randomly oriented grains. If TC (002)  $\approx 1$  for all hkl planes considered, then the films are with randomly oriented crystallite, while values higher than 1 indicate the abundance of grains in a given (hkl) direc-

tion. The values  $0 < TC(hkl) < 1$  indicates the lack of grains oriented in that direction. As  $TC(hkl)$  increase, the preferential growth of the crystallites in the direction perpendicular to the  $hkl$  plane is the higher. The variation of  $TC(002)$  of films with respect to temperature and concentration is shown in Figure 2 and Figure 3. It can be seen that at  $300^{\circ}\text{C}$  deposition temperature there is no orientation of grains along  $c$ -axis, as temperature increases  $c$ -axis orientation increases.  $TC(002)$  has its maximum value at  $400^{\circ}\text{C}$  and this trend is repeated for all concentrations.

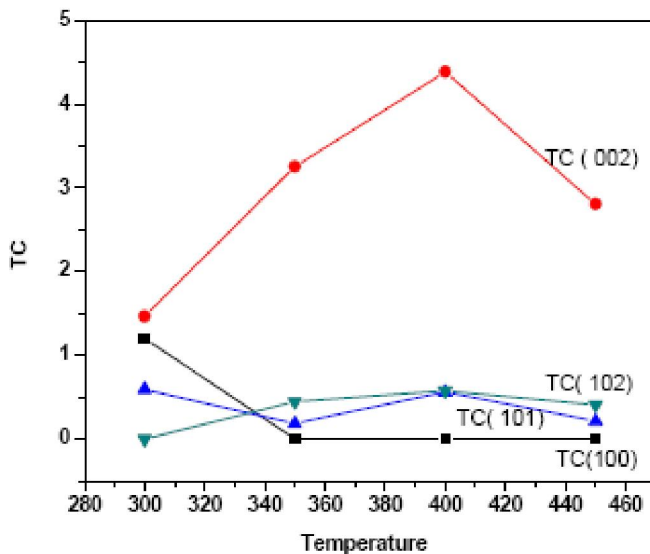


Figure 2 : Texture coefficient Of various planes at different substrate temperatures

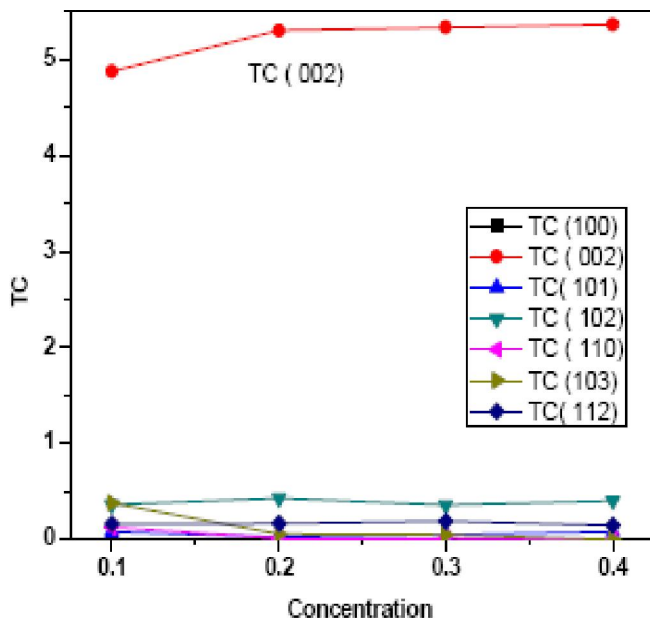


Figure 3 : Texture coefficient Of (002) plane at different solution concentration

To investigate the effect of the substrate temperature on the stress in the ZnO thin films, the stress was calculated using formula

$$\sigma = -453.6 \times c - \frac{c_0}{c} \quad (5)$$

Where  $c_0$  ( $5.206 \text{ \AA}$ ) is the  $c$ -axis lattice constant of bulk ZnO and  $c$  is the  $c$ -axis lattice constant calculated from the XRD pattern. From data (TABLE 2.) we confirm that stress is compressive as compared to the value of bulk ZnO. This result indicates that the deposition temperature strongly affects the stress of the ZnO thin films<sup>[34]</sup>.

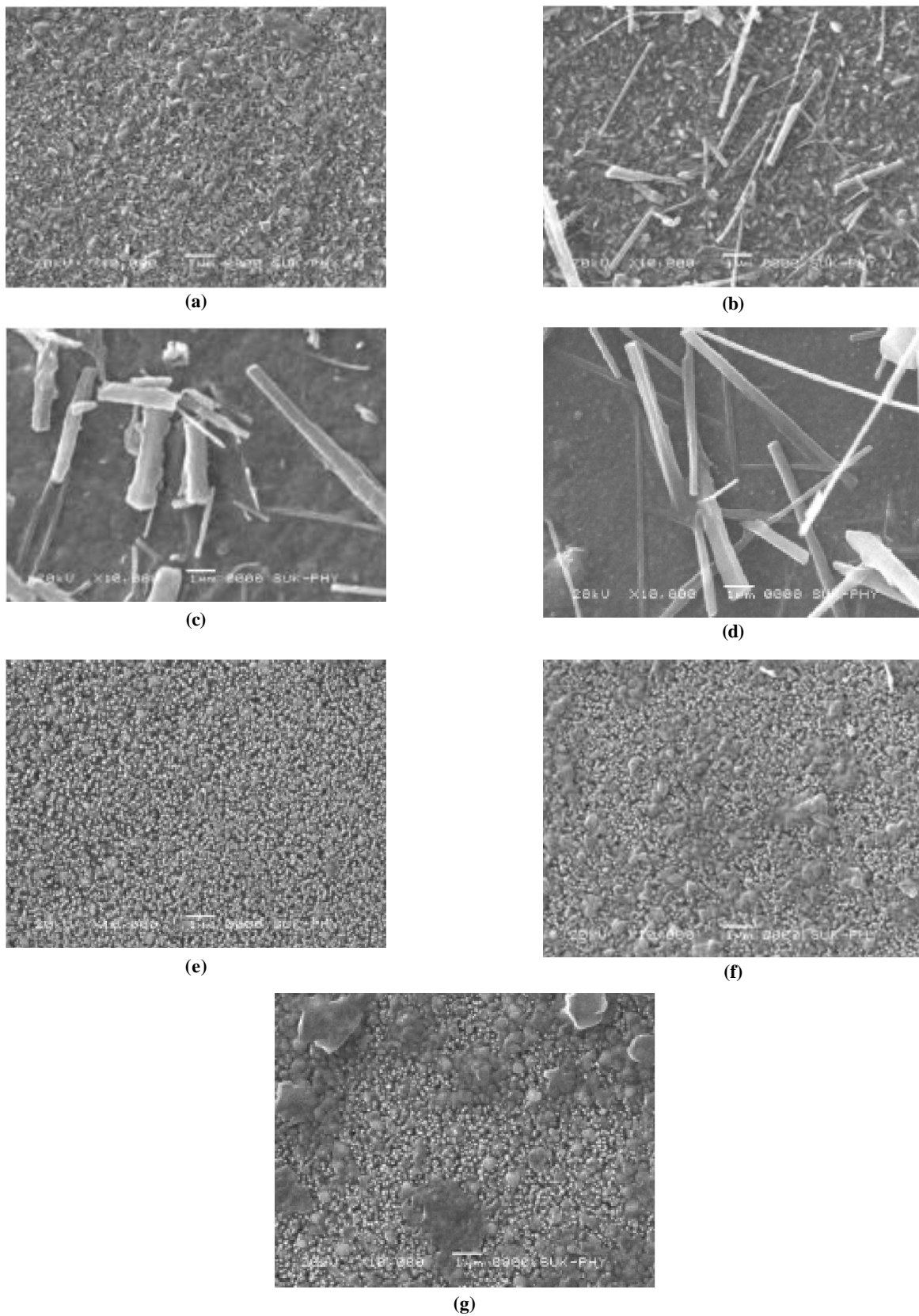
### Morphological studies

The surface topology of the synthesized ZnO rods examined by the SEM is shown in Figure 4. These SEM images show that at  $300^{\circ}\text{C}$  and of  $0.2 \text{ M}$  concentration of zinc acetate, no rods are observed but at higher temperatures  $350^{\circ}\text{C}$  to  $450^{\circ}\text{C}$ , we observed microrods in the plane of film surface, which is agreed with XRD results. As temperature increases diameter of rod increases from about  $0.1 \mu\text{m}$  to  $0.9 \mu\text{m}$  although few thinner rods about  $0.1 \mu\text{m}$  in diameter are seen and length of the rod increases from  $1 \mu\text{m}$  to  $8 \mu\text{m}$ . As temperature and concentration increases, rods becomes regular and almost perpendicular to the substrate, indicating that ZnO microrods preferentially grow along the (002) direction. Similar studies were reported by<sup>[35]</sup>, but we could achieve longer microrods observed in the present case.

### Optical properties

Optical transmission spectra of ZnO Microrods are shown in Figure 5 and Figure 6. The films are uniform and transparent. This is also confirmed by the transmittance spectra of the films. The developed interference pattern in the transmittance shows that the films are specular to a great extent. The average transmittance of the films in the visible region is about 85 % those are deposited at  $400^{\circ}\text{C}$  and  $0.2 \text{ M}$  concentration, which is agree with pervious work reported<sup>[35]</sup>. Also we observed that for higher concentration transmittance goes on decreasing (Figure 6.).

For the direct transition, the optical band gap energy of ZnO thin film was determined by using the equation,

**Full Paper**

**Figure 4 : Scanning Electron micrographs of ZnO thin films (a)300°C, 0.1M, (b) 350°C, 0.1M, (c) 400°C, 0.1M, (d) 450°C 0.1M (e) 400°C, 0.2M (f) 400°C, 0.3M and (g) 400°C, 0.4M**

TABLE 2 : Stress in Gpa at different temperatures and concentrations.

Temperature	Stress in Gpa at 0.1M Conc.	Stress in Gpa at 0.2M Conc.	Stress in Gpa at 0.3M Conc.	Stress in Gpa at 0.4M Conc.
300°C	55.066	4.469	26.801	1.0455
350°C	28.80	-0.48798	0.3485	1.3069
400°C	0.2613	0.4182	0.522	0.7841
450°C	2.2624	0.1394	-87.160	0.7841

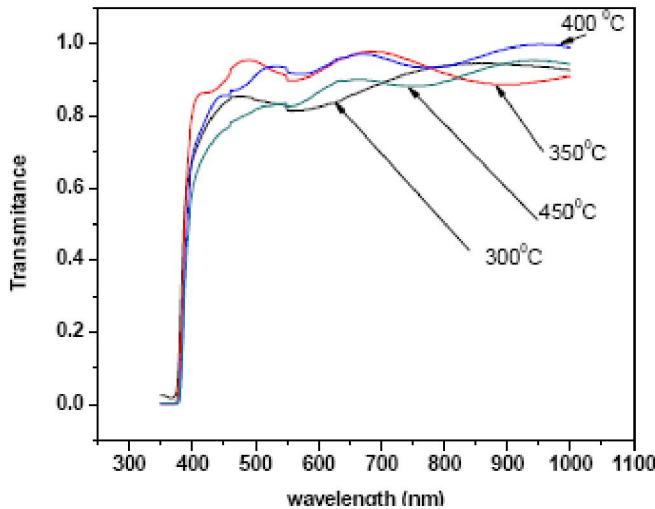


Figure 5 : Transmittance spectra of ZnO thin films at different substrate Temperatures

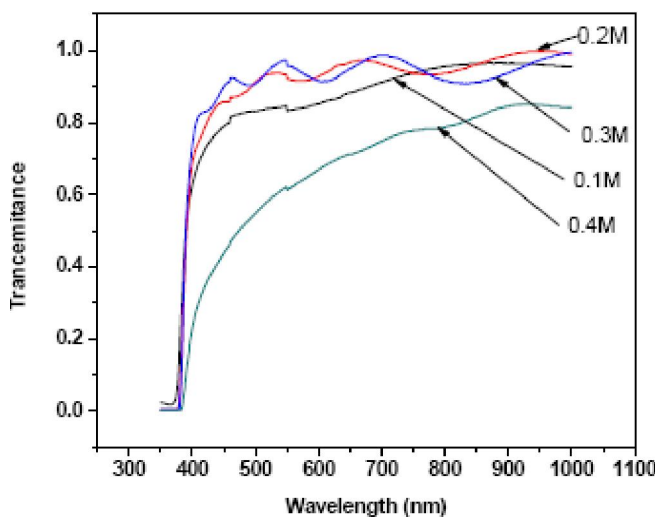


Figure 6 : Transmittance spectra of ZnO thin films at different solution concentrations

$$\alpha = \text{Const.} \frac{(\hbar\nu - E_g)^{\frac{1}{2}}}{\hbar\nu} \quad (6)$$

Where  $\hbar\nu$  is the photon energy and  $E_g$  is the optical band gap which could be calculated from  $(\alpha\hbar\nu)^2$  versus  $\hbar\nu$  plot, which are shown in Figure 7 and Figure 8. By

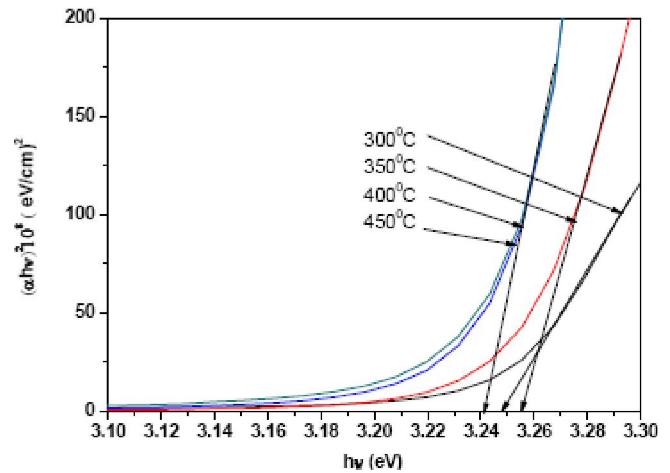


Figure 7 : Plot of  $(\alpha\hbar\nu)^2$  vs  $\hbar\nu$  of ZnO thin films at different substrate Temperatures

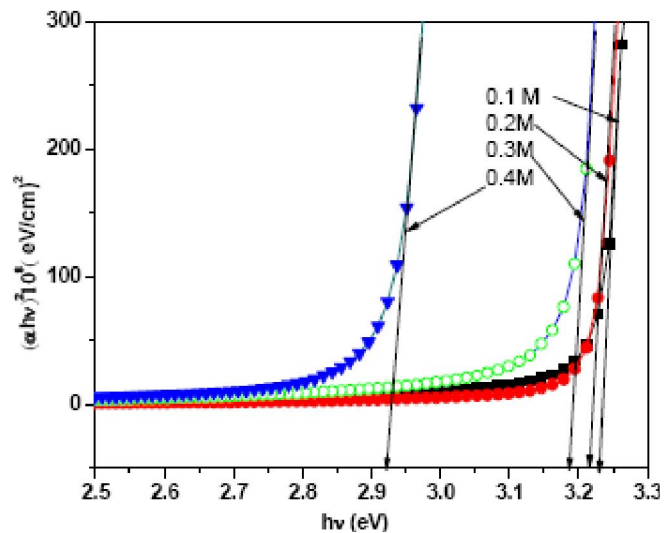


Figure 8 : Plot of  $(\alpha\hbar\nu)^2$  vis  $\hbar\nu$  of ZnO thin films at different solution concentrations

extrapolating the linear part of the plot to  $\alpha = 0$ , optical band gap was estimated. From Figure 7, it is observed that as deposition temperature increases band gap increases, it becomes maximum (3.224 eV) at temperature 400°C and for higher temperature it is slightly decreases. Also it is indicated that from Figure 8, as concentration increases optical band gap decreases considerably due to increases in grain size compared to variation in temperature.

## CONCLUSION

Zinc Oxide (ZnO) microrod thin films of various thicknesses have been obtained by varying deposition temperature and concentration of precursor. All the films except deposited at 300°C showed c- axis growth per-

## Full Paper

pendicular to substrate surface. At a substrate temperature 400°C and 0.2 M concentration, ZnO thin film showed the highest (002) peak. The grain size increases (72.26 nm to 105.33 nm) as temperature increases. Zn – O bond length is minimum at 400°C and 0.2M concentration. Dislocation density the films changes from  $1.863 \times 10^{-4} \text{ (nm)}^{-2}$  to  $0.9032 \times 10^{-4} \text{ (nm)}^{-2}$ . Morphological study showed surface microrods are obtained at low concentration (0.1M). Length and diameter of surface microrods were found in the range from 1 μm to 8 μm and 0.1 μm to 0.9 μm respectively. Optical band gap of ZnO thin films was found to be in the range 2.92 eV to 3.24 eV. The films are compressive comparative to bulk ZnO with average transmission is of the order of 85% in the visible region.

### REFERENCES

- [1] A.Othomo, M.Kawasaki; Appl.Phys.Lett., **75**, 980 (1999).
- [2] L.Zhiefeng, Y.Jing, E.Lei; Solid State Electrochem, **14**, 957 (2010).
- [3] B.Wacogne, M.P.Roe, T.A.Pattinson ; Appl.Phys.Lett., **67**, 1674 (1995).
- [4] A.Barker, S.Crowther, D.Rees; Sens.Actuator.A., **58**, 229 (1997).
- [5] Y.Wu, H.Yan, M.Huang, B.Messer, J.H.Song, P.Youg; Chem.Eur.J., **8**, 1260 (2002).
- [6] R.Konenkamp, R.C.Word, C.Schlegel; Appl.Phys.Lett., **85**, 6004 (2004).
- [7] D.A.Lamb, S.J.C.Irvine; J.Cryst.Growth., **273**, 111 (2004).
- [8] R.Martins, E.Fortunato, P.Nunes, I.Ferreira, A.Marques; J.Appl.Phys., **96**, 1398 (2004).
- [9] B.K.Meyer, H.Alves, D.M.Hofmann, W.Kriegesis, D.Forster, F.Bertam, J.Christen, A.Hoffmann, M.Strai Bburg, M.Dworzak, U.Haboeck, A.V.Rodina; Phys.Status Solids, B.Basic Res., **241**, 231 (2004).
- [10] P.Tonto, O.Makasuwandu Mrong, S.Prasearthdan; Ceramic International, **34**, 57 (2008).
- [11] T.Dedova, O.Volobujeva, J.Klauson, A.Mere, M.Krunles; Nanoscale Res.Lett., **2**, 391 (2007).
- [12] M.Y.Ge, H.P.Wu, L.Ninu, J.F.Liu, S.Y.Chen, P.Y.Shen, Y.W.Zeng, Y.W.Wang, G.Q.Zhang, J.Z.Jiang; J.Crystal Growth, **3056**, 162 (2007).
- [13] U.Alver, T.Kiline, E.W.Bacaksiz, T.Kucukomerog, W.S.Nezir, I.H.Muttu, F.Aslan; Thin Solid Films, **515**, 3448 (2007).
- [14] X.Q.Meng, D.X.Zhao, T.Y.Zhang, D.Z.Shen, Y.M.Lu, Y.C.Liu, X.W.Fan; Chem.Phys.Lett., **407**, 91 (2005).
- [15] Z.W.Pal, Z.R.Dai, Z.L.Wang; Science, **291**, 1947 (2001).
- [16] A.Umar, S.Lee, Y.S.Lees, K.S.Nahm, Y.B.Hahn; J.Cryst.Growth., **277**, 479 (2005).
- [17] W.Chiou, W.Wu, J.Ting; Diamond Relat Mater, **12**, 1841 (2003).
- [18] K.Keis, E.Magnusson, H.Lindstrom, S.E.Lindauist, A.Hagfeldt; Sol.Energy, **73**, 51 (2002).
- [19] M.H.Huang, Y.Wu, H.Feick, N.Tran, E.Weber, P.Yang; Adv.Mater., **13**, 113 (2001).
- [20] Z.R.Dai, Z.W.Pan, Z.L.Wang; Adv.Funct.Mater., **13**, 9 (2003).
- [21] S.E.Ahn, J.S.Lee, H.Kim, B.H.Kang, K.H.Kim, G.T.Kim; Appl.Phys.Lett., **84**, 5022 (2004).
- [22] Y.Sun, G.M.Fuge, M.N.R.Ashfold, Chem.Phys.Lett., **396**, 21 (2004).
- [23] Y.C.Wang, M.Hon; Electrochem Solid State Lett., **5**, 53 (2002).
- [24] W.Li, D.S.Mao, Z.H.Zheng, X.Wang, X.H.Liu, S.C.Zou, Y.K.Zhu, Q.Li, J.F.Xu; Surf.Coat.Technol., **128**, 346 (2000).
- [25] A.R.Babar, P.R.Deshamukh, R.J.Deokate, D.Haranath, C.H.Bhosale, K.Y.Rajpure; J.Phys.D.Appl.Phys., **41**, 135404 (2008).
- [26] F.Paraguay, D.W.Estrada L.D.R.Acosta, N.E.Andrade, M.Miki-Yoshida; Thin Solid Films, **350**, 192 (1999).
- [27] Y.Hong, G.M.Choi; Sensors and Actuators.B., **55**, 47 (1999).
- [28] B.Joseph, K.G.Gopohandran, P.K.Manoj, P.Koshy, V.K.Vaidyan; Bull.Mater.Sci., **22**, 921 (1999).
- [29] H.Gomez, L.Mdela; Mater.Sci.Eng.B., **134**, 20 (2006).
- [30] J.Y.Lee, D.J.Lim, D.G.Yang; J.Thin Solid Films, **515**, 6094 (2007).
- [31] F.Callaud, A.Smith, J.F.Baumard; J.Eur.Ceramics., **6**, 313 (1999).
- [32] X.S.Wang, Z.C.Wu, J.F.Webb, Z.G.Liu; Appl.Phys.A., **77**, 561 (2003).
- [33] S.Ilican, Y.Caglar, M.Caglar; J.Optoelectronics and Adv.Materials., **10**, 2578 (2008).
- [34] S.J.Kang, Y.H.Joung, H.H.Shin, Y.S.Yoon; J.Mater Sci.Mater.Electron., **19**, 1073 (2008).
- [35] U.Ayer; Thin Solid Films, **515**, 3448 (2007).